

Supplementary Material

Structure and mechanics of the human Nuclear Pore Complex basket

Received 00th January 20xx,
Accepted 00th January 20xx

DOI: 10.1039/x0xx00000x

Anthony Vial^a, Luca Costa^a, Patrice Dosset^a, Pietro Rosso^a, Gaëlle Boutières^a, Orestis Faklaris^b,
Heiko Haschke^c, Pierre-Emmanuel Milhiet^{a*} & Christine M. Doucet^{a*}

^a CBS (Centre de Biologie Structurale), Univ Montpellier, CNRS, INSERM, Montpellier, France.

^b MRI, Biocampus, University of Montpellier, CNRS, INSERM, Montpellier, France.

^c Bruker Nano GmbH, Berlin, Germany.

*Corresponding authors: pem@cbs.cnrs.fr, christine.doucet@cbs.cnrs.fr

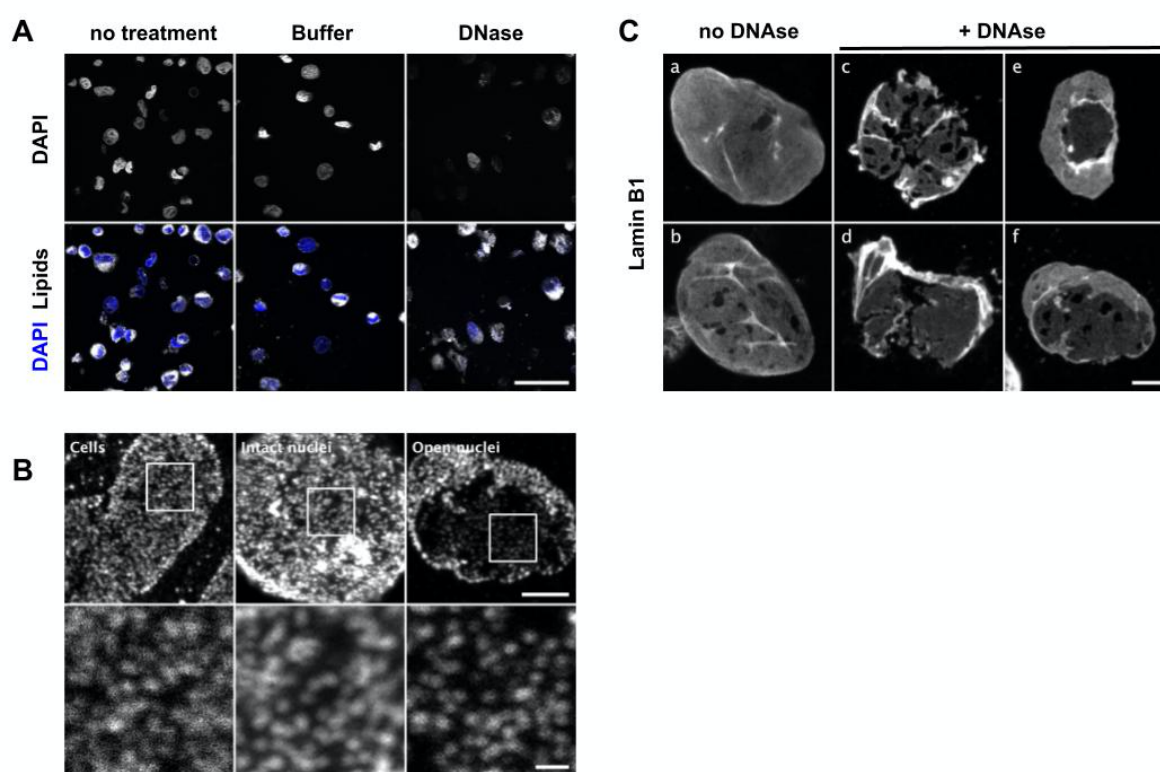


Fig. S1. Supplementary information for figure 1

A- Confocal images of nuclei extracted from U2OS and treated or not with nucleases or buffer. Samples were labelled with Hoechst (blue) and a lipid dye (DiOC6, grey scale) and imaged by confocal microscopy. Scale bar is 50 μm . B- Confocal images of cells, nuclei and nuclear envelopes labelled with mAb414. The boxed areas are zoomed in the lower panel. Scale bars are 5 μm (top) and 1 μm (bottom). C- Confocal imaging of nuclei treated (c-f) or not (a-b) with nucleases and labelled with anti-lamin B1. Well-circumscribed openings (e) better preserve membrane integrity, as depicted by homogenous lamin staining; scale bar is 5 μm .

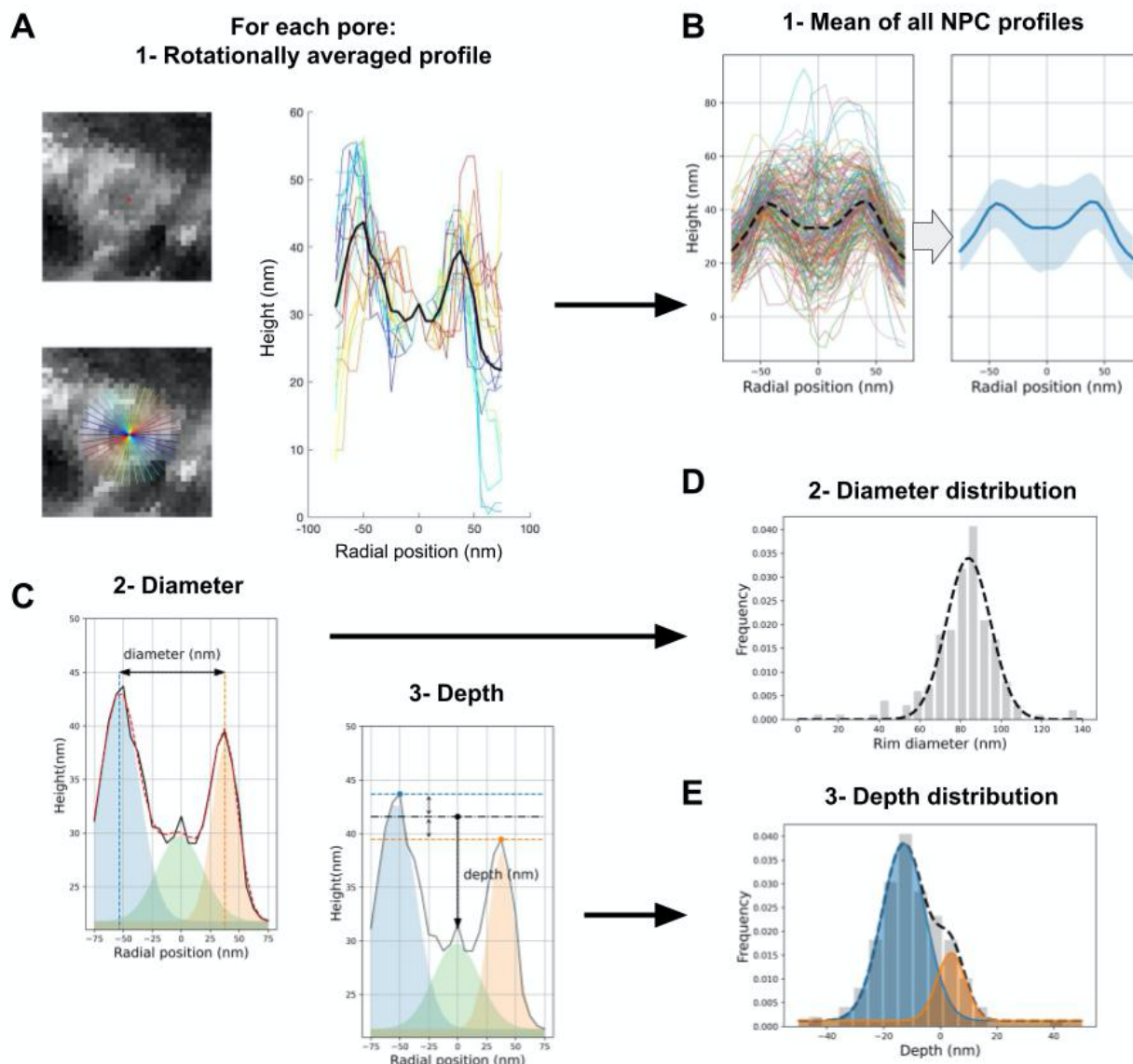


Figure S2. Supplementary information for figure 2

A- Individual pores are manually cropped from $2\mu\text{m} \times 2\mu\text{m}$ AFM scans. For each pore, a height profile is measured along a 150 nm-line drawn across pore center. The line is then rotated 0.05π up to π and a profile is generated at each angle. The 20 profiles are then averaged to produce a single rotationally averaged height profile per pore (black line). B- The profiles of >200 pores were averaged to show the mean height profile of NPCs (right panel, the shaded area corresponds to the standard deviation). C- Pore diameter and depth are calculated from individual rotationally averaged height profiles: each profile is fitted with three gaussians; the diameter is the distance between the first and last gaussian peaks (corresponding to the ring position). The depth is calculated as the height difference between the pore center (radial position = 0) and the average ring height. Depths are thus positive in protruding pores and negative in collapsed ones. D-E- Diameter and depths distributions of >200 NPCs are then plotted as frequencies and fitted with one (respectively two) gaussians. The dashed line represents the fit function. These graphs are also shown in figure 2G & H.

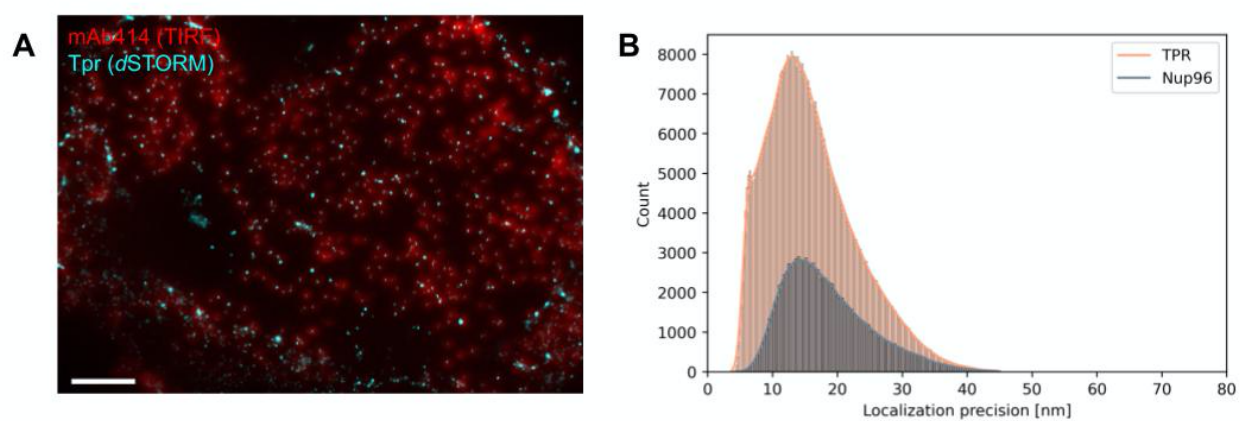


Figure S3. Supplementary information for figure 3

A - Composite image of a NE labeled with mAb414 coupled to Alexa Fluor 594 and anti-Tpr detected with an anti-Rabbit coupled to Alexa Fluor 647. The TIRF image of the 594 channel is merged with the reconstructed map of the *d*STORM acquisition in the 647 channel. Scale bar is 2 μ m.

B - Distribution of *d*STORM localization precision for Tpr and Nup96 labelled with Alexa Fluor 647. Data were extracted from 2 typical images.

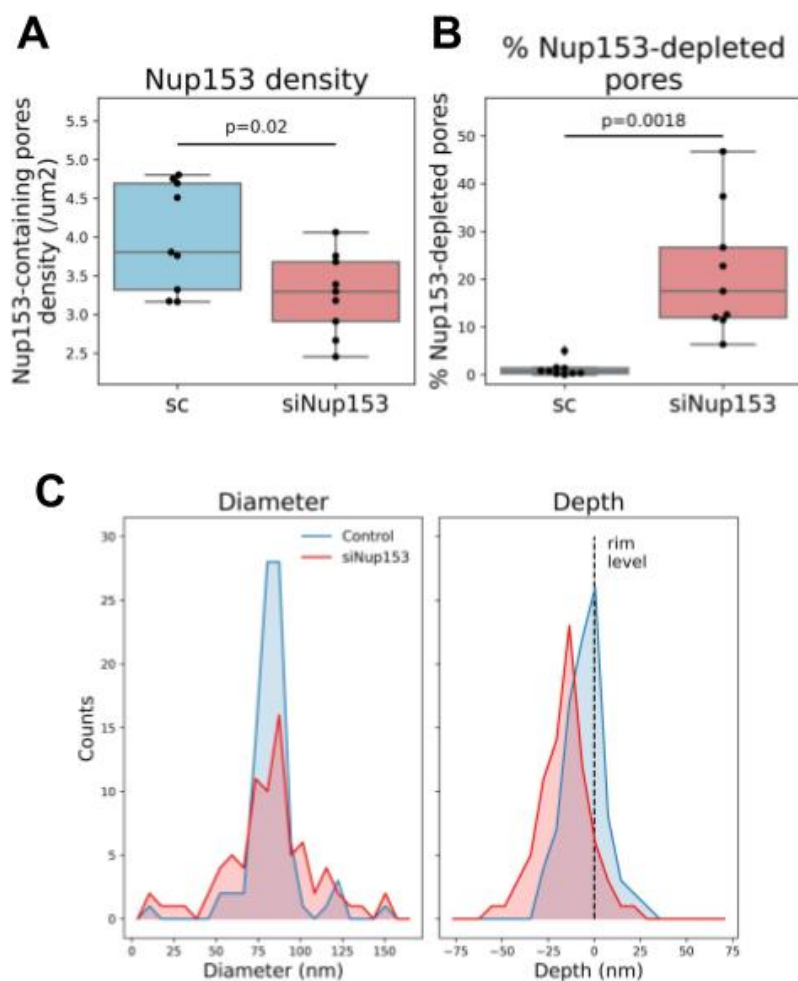


Figure S4. Supplementary information for figure 4

U2OS/GFP-Nup96 cells were treated with scrambled or Nup153-specific siRNAs. The density of pores positively labeled with anti-Nup153 was counted for 9 nuclei in each condition (A). From the same nuclei we calculated the percentage of pores (= Nup96+) with no detectable Nup153 labeling (B).

C- NPC diameter and depth were measured from rotationally averaged height profiles of over 80 pores from control or Nup153-depleted nuclei.

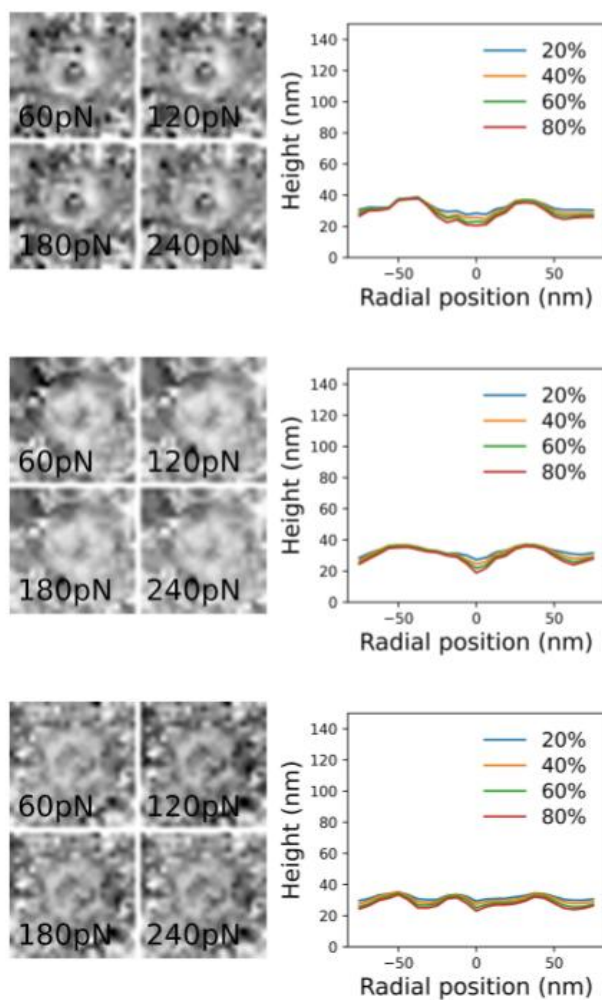


Figure S5. Supplementary information for Figure 5

Topography images of individual pores reconstructed at 60, 120, 180 and 240 pN with their corresponding rotationally averaged height profiles.